J Mol Model (2012) 18:5005–5016
DOI 10.1007/s00894-012-1496-y

ORIGINAL PAPER

Investigation of H-bonding and halogen-bonding effects in dichloroacetic acid: DFT calculations of NQR parameters and QTAIM analysis

Mehdi D. Esrafili

Received: 29 December 2011 / Accepted: 6 June 2012 / Published online: 27 June 2012

Abstract A theoretical study was performed to examine hydrogen and halogen bonds properties in gas phase and crystalline dichloroacetic acid (DCAA). The specific pattern of O–H···O, C–H···O, HCl, Cl···O and Cl···Cl interactions in DCAA dimers is described within the quantum theory of atoms in molecules (QTAIM) formalism. Based on QTAIM results, a partial covalent character is attributed to the O–H···O hydrogen bonds in DCAA, whereas all the C–H···O, Cl···O and Cl···Cl intermolecular interactions are weak and basically electrostatic in nature. MP2/6-311++G** calculations indicate that the interaction energies for DCAA dimers lie in the range between -0.40 and -14.58 kcal mol^{-1}. One of the most important results of this study is that, according to energy decomposition analyses, halogen bonds are largely dependent on both electrostatic and dispersion interactions. For those nuclei participating in the hydrogen-bonding and halogen-bonding interactions, nuclear quadrupole coupling constants exhibit significant changes on going from the isolated molecule model to the crystalline DCAA. Of course, the magnitude of these changes at each nucleus depends directly on its amount of contribution to the interactions.

Keywords Dichloroacetic acid · Halogen bond · Hydrogen bond · NQR · QTAIM

M. D. Esrafili (✉)
Laboratory of Theoretical Chemistry, Department of Chemistry, University of Maragheh,
P.O. Box: 5513864596, Maragheh, Iran
e-mail: esrafili@maragheh.ac.ir

Introduction

In recent years, considerable attention has focused upon the issue of noncovalent interactions due to their essential role in structures and stabilities of a broad range of molecular complexes and crystals [1, 2]. The hydrogen bond (HB), the chief mode of interaction of which is through electrostatic and charge-transfer (delocalization) forces, has been the subject of many investigations and it is believed to be the best characterized type of noncovalent interactions [3–6]. The HB is most frequently defined as an X–H···Y interaction, where X and Y are electronegative elements and Y possesses one or more lone electron pairs. There are also so-called unconventional HBs such as C–H···Y, X–H···C, X–H···π -electrons or even C-H···C [7]. One can also mention dihydrogen bonds, a special kind of HB where the negative charged H-atom is a proton acceptor [8]. Besides the HB, there are also other important noncovalent interactions. A halogen bond is a short-range RX···YZ interaction, where X is a halogen (typically chlorine, bromine, or iodine) that is part of the molecule RX and YZ is a Lewis base; Y is often an atom, such as oxygen, nitrogen, or sulfur, that has a lone pair [9, 10]. Halogen bonds share many physical properties with the more commonly encountered HBs [11, 12] and Sandorfy et al. have shown via infrared spectra that the former can compete and interfere with the latter [13, 14]. It is increasingly recognized that halogen-bonding plays a critical role in a wide variety of biochemical phenomena such as protein-ligand complexation [15–17], and can be utilized effectively in drug design. Another area of application is crystal engineering; [15] co-crystals can be produced that have specific desired features of structure and composition, leading to, for example, non-linear optical activity and enhanced conducting properties.

Considering the fact that halogen atom (X) as well as halogen bond electron donor (Y) atoms are negatively charged, the existence of halogen bonds is surprising. The problem was clarified by Auffinger et al. [18], Politzer et al. [19], and Clark et al. [20] who showed the existence of an electropositive crown called the " σ-hole " at the top of the halogen atom directed toward the electron donor (Y). Experimental results [21–23] and theoretical calculations [24–26] consistently show that the greater the polarizability and the lower the electronegativity of a halogen atom, the more positive is its σ-hole and the stronger is the halogen bond to which it gives rise. The strength of halogen bond formed by a halogen derivative with a given electron rich moiety (halogen bond acceptor) thus decreases in the order I> Br>Cl. As a result of a combination of extreme electronegativity and limited polarizability, the F atom is frequently deemed to not participate in halogen-bonding. The electron density distribution around F is nearly spherical rather than anisotropic and consequently, F is most likely to behave as halogen bond acceptors. However, it has recently been shown that fluorine atom has the capability of forming halogen bonds and can also affect recognition and self assembly processes, but only under specific circumstances [27, 28]. Like H-bonded complexes, halogen-bonded complexes were originally classified as charge-transfer complexes in which the charge-transfer is considered to be the dominant factor in determining the complex structure [29]. However, the consideration of only the charge-transfer interaction may not be sufficient in describing the ground-state stabilization of halogen-bonding complexes. On the other hand, the electrostatic effect, polarization, charge-transfer, and dispersion contributions all play an important role. Recently, Hobza and coworker [30] showed that halogen bonds are largely dependent on both electrostatic and dispersion type interactions. As the halogen atom involved in halogen-bonding becomes larger the interaction strength also gets larger and, interestingly, more electrostatic (and less dispersive) in character.

Dichloroacetic acid (DCAA) exhibits various short-range HB as well as halogen-bond interactions in solid phase. Recently, Gajda and Katrusiak [31] carried out a crystallographic database survey of O–H···O, Cl···O and Cl···Cl short intermolecular contacts in DCAA crystals and found that the latter one contributes to the formation of a specific triangular Cl_3 pattern. The authors showed that the crystal structure of DCAA is mainly governed by hydrogen-bonding (H–bonding) the molecules into dimers and by halogen···halogen interactions. In this work, we performed a theoretical study at a reliable level of DFT and MP2 calculations on HBs and halogen-bonding properties in both gas phase and crystalline DCAA. This system is selected to mimic halogen-bonding found within gas phase and crystal structures as well as within biological molecules. Such a theoretical study may provide some valuable information of the origin and strength of halogen-bonding interactions, which would be very important for the design and synthesis of new materials and effective drugs containing halogenated compounds.

Computational details

All molecular orbital calculations were performed using GAMESS electronic structure package [32]. The geometries for all stationary points have been optimized using the 6-311++G** basis set. The inclusion of diffuse functions in the basis is a clear requirement to adequately describe H-bonded or halogen-bonded systems [33]. We examined the ability of six density functionals [including one hybrid GGA (B3LYP), one meta–GGA (M06-L), two hybrid meta-GGA (M06, M06-2X) and two long-range corrected functionals (CAM-B3LYP and wB97XD)] to evaluate the binding distances and optimized structures. Zhao and Truhlar have recently developed the M06 family of local (M06-L) and hybrid (M06, M06-2X) meta-GGA functionals that show promising performance for noncovalent interactions [34]. The interaction energies of all DCAA dimers have been computed as the differences between the total energies of the dimers and the energies of the isolated monomers and have been corrected for basis set superposition error (BSSE) using the counterpoise method [35]. The topological calculations of quantum theory of atoms in molecules (QTAIM) [36] were performed using the GAMESS program [32], but the molecular graphs used for interpretation of charge density were generated using AIM 2000 software [37].

In order to analyze various HBs and halogen bonds interactions in terms of meaningful physical components, interaction energies were decomposed using Kitaura-Morokuma method as [38]:

$$E_{\text{int}} = E_{EL}^{(1)} + E_{EX}^{(1)} + E_{DEL}^{(R)} + E_{DISP} \quad (1)$$

where $E_{EL}^{(1)}$ is the first-order electrostatic term describing the classical columbic interaction of the occupied orbitals of one monomer with those of another monomer, $E_{EX}^{(1)}$ is the repulsive first-order exchange component resulting from the Pauli exclusion principle, $E_{DEL}^{(R)}$ and E_{DISP} correspond to higher order delocalization and dispersion terms. The delocalization term contains all classical induction, exchange-induction, etc., from the second order up to infinity. All energy components were calculated using GAMESS package [32].

The crystalline structures of DCAA were available from X-ray [31]. Since the positions of hydrogen atoms are not located accurately by X-ray diffraction, a geometry optimization of just the hydrogen atoms in the structure was needed. In the present study, partial geometry optimizations were carried out using B3LYP, M06-L, M06, M06-2X,

CAM-B3LYP and wB97XD with 6-311++G** standard basis set.

In nuclear quadrupole resonance (NQR) spectroscopy, the interaction between nuclear electric quadrupole moment and electric field gradient (EFG) at quadrupole nucleus is described with Hamiltonian as follows [39]:

$$\hat{H} = \frac{e^2 Q q_{zz}}{4I(2I-1)}\left[\left(3\hat{I}_z^2 - \hat{I}^2\right) + \eta_Q\left(\hat{I}_x^2 - I_y^2\right)\right], \quad (2)$$

where eQ is the nuclear electric quadrupole moment, I is the nuclear spin, and q_{zz} is the largest component of the EFG tensor. The principal components of the EFG tensor, q_{ii}, are computed in atomic unit ($1\ au = 9.717365 \times 10^{21}\ V\,m^{-2}$), with $|q_{zz}| \geq |q_{yy}| \geq |q_{xx}|$ and $q_{xx}+q_{yy}+q_{zz}=0$. These diagonal elements relate to each other by the asymmetry parameter: $\eta_Q = |q_{yy} - q_{xx}| / |q_{zz}|$, $0 \leq \eta_Q \leq 1$, that measures the deviation of EFG tensor from axial symmetry. The computed q_{zz} component of EFG tensor is used to obtain the nuclear quadrupole coupling constant from the equation; $C_Q(\mathrm{MHz}) = e^2 Q q_{zz}/h$, using the recently reported value for the ^{2}H, ^{35}Cl and ^{17}O electric quadrupole moments of 2.86, -81.65 and -25.58 mb, respectively [40].

Results and discussion

The possibility of HBs and halogen bonds formation between the DCAA monomers in the gas phase will be discussed first. Geometries, interaction energies and topological analyses of the stable DCAA dimers performed at different computational levels will be presented. Then, a comparison of HBs and halogen bonds characteristics in crystalline DCAA is presented based on the evaluated NQR parameters. Here we evaluate the role of intermolecular interactions in the solid lattice, and we seek to find the main factors that differentiate calculated NQR parameters at the sites of the various nuclei. Unless otherwise noted, the following results are referred for the M062X/6-311++G** level of theory.

Isolated dimers

Electrostatic potential and geometries

We will look first at the overall electrostatic potential on the surface of DCAA molecule. For this purpose, we compute electrostatic potential on the molecular "surface" which we define, following Bader et al. [41] as the 0.001 electrons/bohr^3 contour of the electronic density ρ(r) [42, 43]. This surface potential is labeled $V_{S(r)}$. The graphical illustration of the $V_{S(r)}$ for the DCAA monomer is shown in Fig. 1. As would be anticipated, the most negative electrostatic potential on the DCAA surface is associated with the carbonyl oxygen (O2). On the other hand, the very strongly positive electrostatic potential of the hydroxyl hydrogen (H1), $V_{S,max}$= 60.4 kcal mol^{-1}, and the $V_{S,min}$=-30.2 kcal mol^{-1} of the carbonyl oxygen indicate their propensities for noncovalent H-bonding, as a donor and an acceptor, respectively. Perhaps more surprisingly, there is also a smaller and weaker positive region on the outermost portion of each Cl atom centered about the intersection of its surface with the C–Cl axis. These $V_{S,max}$ are 11.9 kcal mol^{-1} (Cl1) and 10.6 kcal mol^{-1} (Cl2). Such halogen positive region is referred as the "σ-hole", because it is centered on the C–X axis and is surrounded by negative electrostatic potential. This is invoked as the explanation for "halogen bonding," which is a noncovalent interaction between a covalently bound halogen on one molecule and a negative site on another. Thus, it is expected that the stabilities of the DCAA clusters depend upon both the magnitudes of the $V_{S,max}$ and $V_{S,min}$ that give rise to the σ-hole bonding.

Figure 2 indicates the most stable structures and evaluated HBs and halogen bonds distances for DCAA dimers analyzed here. All of these structures are minima on the potential energy surface, as verified by Hessian analysis. Because the O···H sum of the van der Waals (vdW) radii amounts to 2.72 Å [44], the O-H···O distances are within the 1.69–1.91 Å, which are less than to the sum of vdW radii mentioned above. The dimer **D1** exhibits the shortest H-bonding distance (about 1.69 Å) among the systems considered. It can be seen from Fig. 2 that the positive $V_{S(r)}$ region on the hydroxyl hydrogen is interacting with the negative potential on the side of the carbonyl oxygen. This seems to be justified to describe the formation of these interactions as electrostatically driven. The estimated O−H···O angle is 178°, just 2° away from exact linearity. Structures **D2** and **D3** are the next most stable dimers found. Inspection of their geometrical features indicates that there might be two H-bonding interactions, which are highlighted in Fig. 2 as dotted lines. Notice, however, that none of them is linear.

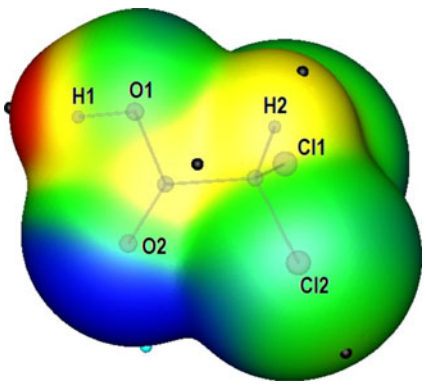

Fig. 1 The electrostatic potential mapped on the surface of DCAA molecular electron density (0.001 e au^{-3}). Color ranges for $V_{S(r)}$, in kcal mol^{-1}: red>37.6, yellow 37.6–15.1, green 15.1– -7.1, blue<-7.1. Black circles surface maxima, blue surface minima

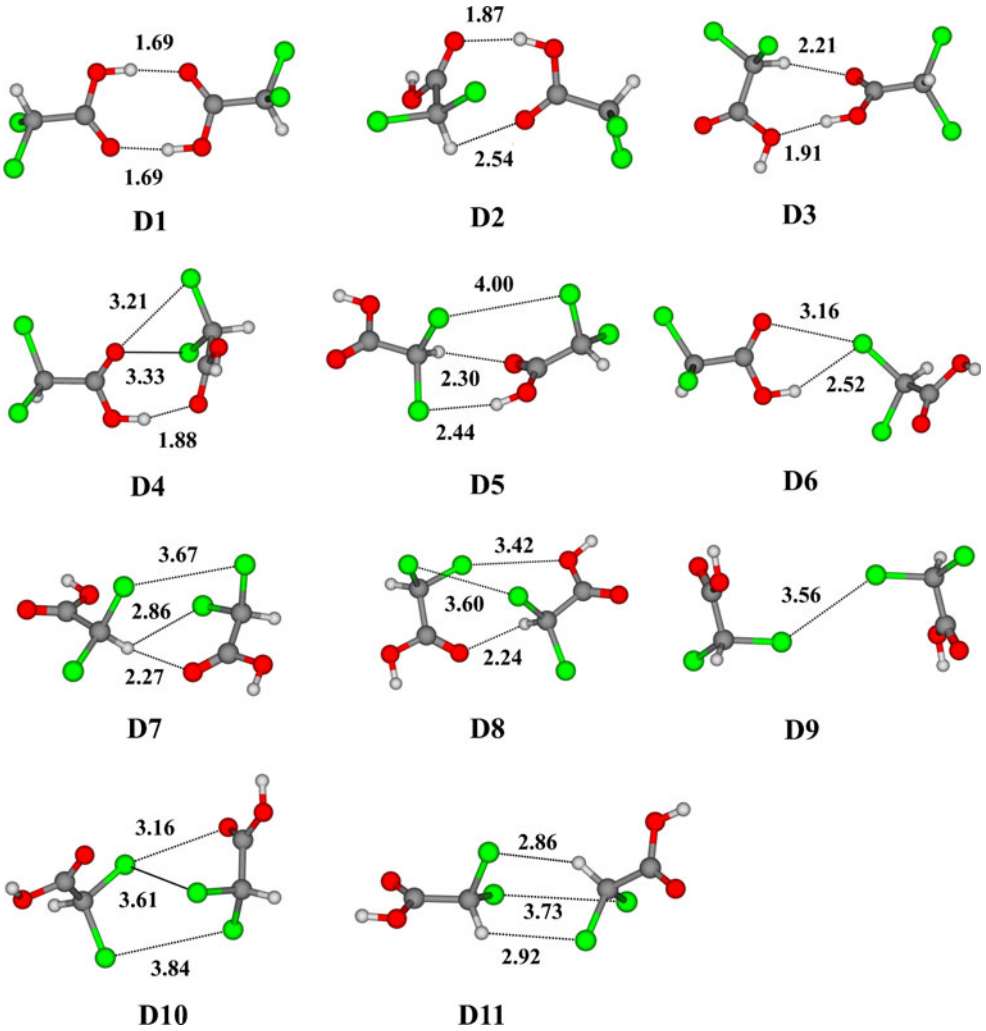

Fig. 2 Gas phase structure of DCAA dimers. The dash lines show intermolecular HB and halogen bond interactions (in Å)

Moreover, remarkable is the long distances between the hydrogens and their corresponding acceptor atoms. For the stronger HB of **D2** and **D3**, that is O···H-O, the O···H distances are 1.87 Å and 1.91 Å, 0.18 Å and 0.22 Å larger than its corresponding distance in structure **D1**, respectively. The weakest HB of **D3** has a CH···O distance of 2.54 which is 0.33 Å larger than its corresponding distance in dimer **D2**. Additionally, we have found one more stable structure involving O-H···O interaction (dimer **D4**). However, this structure is predicted to be less stable than the structures **D2** and **D3**. In this structure, the carboxylic groups lie in planes perpendicular to each other. Notice that the O···H distance has lengthened from 1.69 Å in **D1** to 1.88 Å in **D4**.

The results of geometry optimization show also the existence of H Cl intermolecular contacts for some systems considered here. The H···Cl distances are in the range 2.44-2.92 Å; which amount to or are less than the sums of vdW radii of chlorine and hydrogen atoms. It indicates that according to the geometrical criteria those are attractive HB interactions. The shortest H···Cl distance of 2.44 Å was found at the M062X/6-311++G** level for the **D5** dimer. Inspection of its geometry reveals also the presence of two weak interactions, namely, CH···O and Cl···Cl. The Cl···Cl length, 4.00 Å, of this halogen-bonding is slightly longer than those of other structures. From Fig. 2, it can be seen that one of the positive $V_{S(r)}$ regions on the chlorine, along the extension of the Cl−C bond, is interacting with the negative potential on the side of the chlorine atoms of neighbor molecules. For the DCAA dimers studied here, the evaluated Cl···Cl separations are in a range from 3.56 to 4.00 Å. These separations are slightly longer than the sum of two chlorine vdW radii, 3.50 Å [44]. As mentioned above, the calculated electrostatic potential shows the presence of a positive potential end cap and a negative region on the side of the chlorine atoms. The positive region on the extension of each Cl−C bond is interacting with the negative potential on the carbonyl oxygens; see Figs. 1 and 2. For most of the dimers studied, it has been shown that the optimized equilibrium Cl···O bonds are essentially shorter than the sum of the vdW radii of the Cl and O atoms (3.27 Å) [44], implying an attractive interaction between DCAA monomers.

QTAIM analysis

Previous [45, 46] and recent studies [47–51] reveal that QTAIM is a powerful method for the analysis of HBs and halogen bonds interactions. Generally, for covalent interactions (also known as "open-shell" interactions), the electron density at the bond critical point (BCP), ρ_{BCP}, is large and its Laplacian $\nabla^2\rho_{BCP}$ is negative. On the other hand, for closed-shell interactions (e.g., ionic, van der Waals, or HBs), ρ_{BCP} is small and $\nabla^2\rho_{BCP}$ is positive [36]. However, a clear distinction between the closed-shell and covalent type of interaction is impossible without determination of the local electronic energy density, H_{BCP}. According to Rozas et al. [52], the character of interaction could be classified as function of the H_{BCP} with Laplacian of the electron density at BCP ($\nabla^2\rho_{BCP}$). It means that for strong interactions ($\nabla^2\rho_{BCP}<0$ and $H_{BCP}<0$) the covalent character is established, for medium strength ($\nabla^2\rho_{BCP}>0$ and $H_{BCP}<0$) their partially covalent character is defined, and weak ones ($\nabla^2\rho_{BCP}>0$ and $H_{BCP}>0$) are mainly electrostatic. Thus, the magnitude of H_{BCP} reflects the "degree of covalency" present in a given interaction.

Figure 3 presents molecular graphs for all of the DCAA dimers examined in this work. For both HBs and halogen bonds interactions, there are corresponding bond paths and BCPs within the equilibrium structures. Figure 3 shows the BCPs along the lines joining the Cl/O or two Cl atoms, which establishes the existence of the Cl···O or Cl···Cl halogen-bonding in the DCAA structures, respectively. Table 1 lists the calculated ρ_{BCP}, $\nabla^2\rho_{BCP}$, H_{BCP} and ε values at the H···O, H···Cl, Cl···Cl and Cl···O BCPs. For the O–H···O interactions of **D1**, it can be seen that the values of ρ_{BCP} are calculated to be 0.042 au, whereas the values of $\nabla^2\rho_{BCP}$ are positive (0.142 au). These values are within the common accepted values for H-bonding interactions, thus indicating the closed-shell interactions in DCAA. However, negative values of H_{BCP} are predicted for these HBs, suggesting that the interactions have some degree of covalent character. As is obvious from Table 1, the ellipticity values for the O–H···O interactions are nearly small and zero, indicating that the HBs are conserved in the **D1-D4** structures [53]. Since, the electron density at the BCP is a property which decays exponentially with increasing distance [53]; it may be treated not only as evidence of HB interaction but also as a measure of its strength. For example, for each O–H···O interaction of **D1**, this value amounts to 0.042 au at the M062X/6-311++G** level of theory, and the O···H distance calculated at this level is equal to 1.60 Å; the HB energy for this interaction is about -12 kcal mol^{-1}.

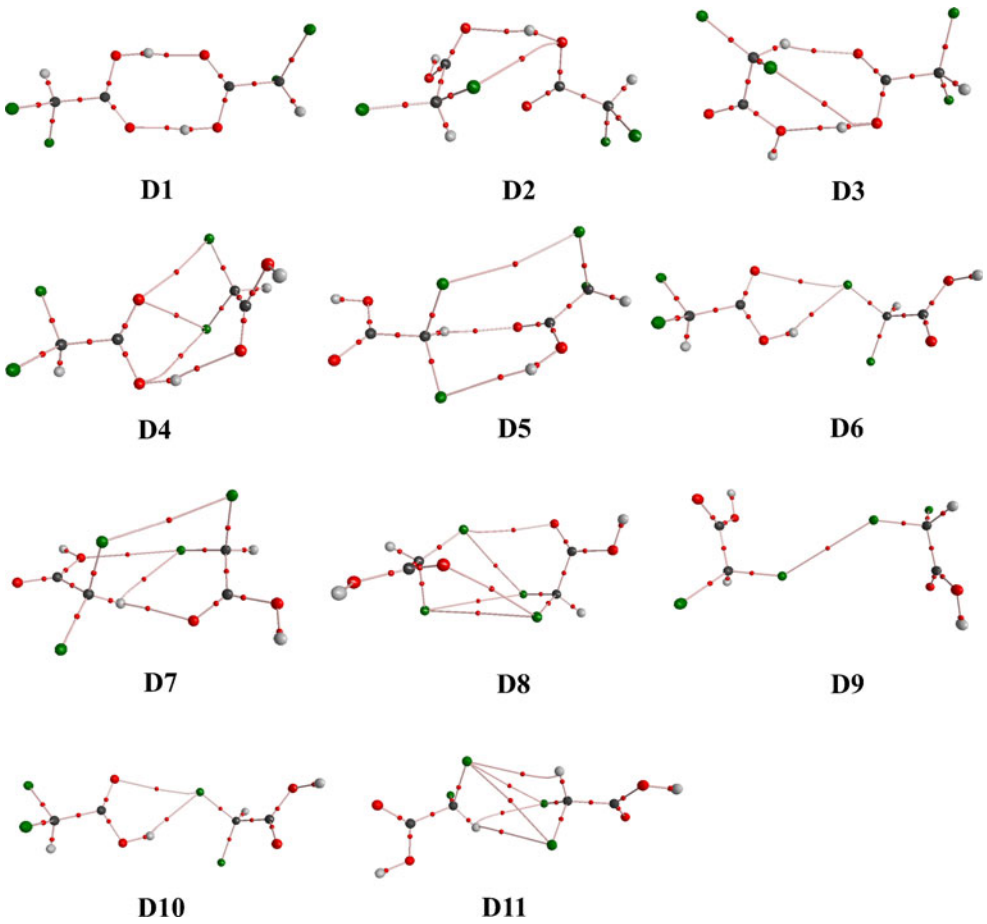

Fig. 3 Molecular graphs of DCAA dimers, solid lines indicate bond paths and large circles correspond to attractors, small red ones to BCPs

Table 1 Topological parameters of ρ for CLAA dimers (electron density at BCP, ρ_{BCP}, its Laplacian $\nabla^2\rho_{BCP}$, total electron energy density (H_{BCP}) and ellipticity (ε) calculated at the M06-2X/6-311++G** level of theory [a]

Dimer	Interaction	ρ_{BCP}	$\nabla^2\rho_{BCP}$	H_{BCP}	ε
D1	O-H···O	0.042	0.142	−0.003	0.014
D2	O2···H1	0.026	0.105	0.002	0.044
	Cl2···O1	0.007	0.028	0.001	1.105
D3	OH···O1	0.024	0.100	0.003	0.076
	O2···HC	0.015	0.058	0.002	0.062
D4	O-H···O	0.026	0.105	0.002	0.045
	O1···Cl2	0.007	0.027	0.001	1.700
	O2···Cl1	0.008	0.030	0.001	0.772
	O2···Cl2	0.007	0.026	0.001	1.322
D5	Cl2···Cl1	0.003	0.010	0.001	1.412
	Cl1···H1	0.013	0.045	0.002	0.031
	CH···O2	0.013	0.051	0.002	0.230
D6	OH···Cl2	0.011	0.040	0.002	0.025
	O2···Cl	0.009	0.031	0.001	0.060
D7	Cl2···Cl1	0.006	0.019	0.001	0.085
	Cl2···Cl2	0.006	0.022	0.001	0.257
	O1···Cl2	0.005	0.020	0.001	0.062
	CH···Cl2	0.007	0.024	0.001	0.233
	CH···O2	0.014	0.053	0.002	0.148
D8	Cl1···Cl2	0.006	0.019	0.001	0.085
	Cl1···Cl1	0.006	0.022	0.001	0.257
	Cl1···O2	0.005	0.020	0.001	0.061
	CH···O2	0.014	0.053	0.002	0.148
	CH···Cl1	0.007	0.024	0.001	0.233
D9	Cl1···Cl2	0.005	0.021	0.001	0.163
D10	Cl1···Cl1	0.006	0.020	0.001	1.469
	Cl1···Cl2	0.006	0.021	0.001	0.784
	Cl···HC	0.007	0.025	0.001	0.331
	CH···Cl1	0.007	0.023	0.001	0.069
	CH···Cl2	0.008	0.026	0.001	0.386
D11	O2···Cl2	0.005	0.019	0.001	0.047
	O2···Cl2	0.005	0.019	0.001	0.047
	Cl1···Cl1	0.004	0.014	0.001	0.026
	Cl2···O2	0.008	0.030	0.001	0.073

[a] All ρ_{BCP}, $\nabla^2\rho_{BCP}$, and H_{BCP} values in atomic units

As pointed out above, the origin of halogen-bonding is connected with formation of the so-called σ-hole, a region of positive electrostatic potential on the outermost region of the halogen atom surface, centered on the extension of the R-X bond [9]. The presence of the σ-hole in some halogen derivatives forming halogen bonds allows one to suspect that this interaction is rather electrostatic in nature [54, 55]. However, it has been reported that interaction between the R-X and Lewis base cannot be simply reduced to electrostatic interaction and that other contributions to the interaction energy are also decisive. As it is obvious from the Table 1, the small values of ρ_{BCP}, the positive values of the $\nabla^2\rho_{BCP}$, the high values of ε and the nearly zero values of H_{BCP} suggest, according to the Rozas [52] criterion, that all Cl···O intermolecular interactions, are weak and basically electrostatic in nature. More specifically, it can be seen that the values of ellipticity obtained for the Cl···O interactions are within the range of 0.047–1.70. Thus, the slightly large value of ellipticity reveals instability of the Cl···O bonds [35]. The existence of Cl···Cl interactions in DCAA dimers is also revealed by the presence of corresponding BCPs in the molecular graphs (Fig. 3). For the Cl···Cl interactions characterized in this work, the values of ρ_{BCP} are calculated to be in a range of 0.003-0.006 au, whereas the values of $\nabla^2\rho_{BCP}$ are all positive, ranging from 0.010 to 0.021 au. The largest value of ρ_{BCP} was found for the structure **D8**, suggesting that this is the strongest. Furthermore, these values are in good agreement with the reported values in the literature for weak halogen-bonding interactions [50, 51].

It is to be noted that there are other intermolecular interactions, in particular, the weak C–H···O and H···Cl, which will have a significant contribution to the energies of packing of the molecules. The topological values of these additional interactions in DCAA dimers are listed in Table 1. Relatively small values of ρ_{BCP}, the positive values of the Laplacian, and values of $H_{BCP}>0$, guarantee the existence of H-bonding and indicate that both C–H···O and H···Cl interactions between DCAA monomers have a significant electrostatic nature. Overall it can be said that, in terms of QTAIM, the weak C–H···O and H···Cl bonds are similar in character to the halogen bonds found in the DCAA dimers.

Interaction energies and EDA

The interaction energy provides a measure of the strength of the interaction between DCAA monomers. Table 2 gives the interaction energies of the DCAA dimers calculated by means of the electron MP2, B3LYP, CAM-B3LYP, M06, M06L, M062X, and wB97XD methods using 6–311++G** basis set. From Table 2, it is found that different theories have important effects on the interaction energies of the DCAA dimers. For **D1** dimer, the order of the interaction energies computed by various theoretical levels is the following: wB97XD>CAM-B3LYP>M06>M06L>M062X>B3LYP>MP2. The interaction energy at the wB97XD level is about ~5 kcal mol^{-1} more negative than that found with the MP2. Considering the halogen-bonded structures discussed above, the B3LYP method greatly underestimates all of the binding energies. This indicates that dispersion must play a large role in the stabilization of DCAA monomers.

Among the DCAA dimers, **D1** with two normal O–H···O= C HBs is the most stable dimer (Table 2). It can be observed that the interaction energy amounts to -14.58 kcal mol^{-1} at the

Table 2 Calculated BSSE-corrected interaction energies for different dimers of DCAA[a]

Dimer	M06	M06L	M062X	B3LYP	CAM-B3LYP	wB97XD	MP2
D1	−18.78	−18.72	−18.66	−17.00	−19.01	−19.24	−14.58
D2	−11.35	−11.83	−12.53	−5.92	−8.53	−10.44	−7.36
D3	−8.20	−8.02	−8.78	−4.71	−6.65	−8.05	−5.92
D4	−9.14	−9.64	−10.24	−4.13	−6.56	−8.26	−5.65
D5	−6.14	−6.48	−6.86	−1.74	−3.54	−5.44	−3.34
D6	−2.91	−3.12	−3.28	−1.21	−2.03	−2.78	−1.85
D7	−4.77	−5.15	−5.33	0.64	−1.35	−3.59	−2.01
D8	−4.82	−5.18	−5.39	0.67	−1.40	−3.64	−2.09
D9	−0.14	−0.29	−0.48	0.22	−0.12	−0.47	−0.40
D10	−3.43	−3.92	−4.18	0.98	−0.54	−2.89	−1.29
D11	−2.51	−2.98	−2.74	3.09	1.37	−0.89	0.44

[a]All binding energies in kcal mol^{-1}

MP2 level for this dimer. All DFT functionals give rather similar results, though interaction energies are slightly greater. These results are in good agreement with the MP2 stabilization energy for acetic acid dimer calculated with aug-ccpVTZ basis set (-15.8 kcal mol^{-1}) [56] and B3LYP/6–31 G** and RI MP2/augTZVPP values (-15.9 kcal mol^{-1}) [57]. On the other hand, the stabilization caused due to HB formation in an improper C–H···O=C bond is almost less significant compared to the classic O–H···O=C bond. Interaction energies are small for the dimers **D2** and **D3** calculated to be -7.36 and -5.92 kcal mol^{-1} at the MP2/6–311++G**, respectively. Contrary to **D1**, these H–bonded dimers are stabilized by nonlinear C–H···O=C interactions with an HB distance of 2.21 and 2.54 Å (Fig. 2). In a prior study of HC≡CH···O3 dimers, it was found that analogous C–H···O HBs, involving only one hydrogen acceptor, gave an average interaction energy -2.92 kcal mol^{-1} [58]. In the case of **D4** and **D5** structures, the evaluated interaction energies are predicted to be -5.65 and -3.34 kcal mol^{-1}, respectively. Recall that **D4** has O-H···Cl and O···Cl type of interactions, while only the weak CH···O and H···Cl ones are present in **D5**. Inspection of Table 2 reveals that the Cl···O and Cl···Cl halogen-bonded dimers of DCAA are also weak.

It is worth comparing halogen-bonded complexes with their hydrogen-bonded counterparts, since competition between these two interactions was often considered previously [30]. For the halogen-bonded structures characterized here, the interaction energy increases from -0.48 to -10.24 kcal mol^{-1}. The interaction strength for the Cl···Cl interaction in **D9** is calculated to be of -0.48 kcal mol^{-1}. What is more, the **D10** structure is about 3.70 kcal mol^{-1} more stable than **D9**. This analysis suggests that despite its weakness, the O···Cl halogen bonds have a great influence on the overall binding energies of DCAA monomers. This result has also been found for other types of halogen bonds [30, 47–51]. This also supports the conclusion that the interaction energy of halogen bonding correlates with the magnitude of the surface electrostatic potential maxima/minima on the donor/acceptor atoms [24, 43].

In order to analyze various HBs and halogen bonds interactions in terms of meaningful physical components, interaction energies were decomposed using Eq. 1. It should be noted here although the most frequently quoted mechanism of halogen bond formation may suggest a significantly electrostatic nature of this interaction, the Kohn–Sham MO approach indicates a significantly covalent character of such interaction [59]. Recently, Palusiak [59] indicated that the HOMO/LUMO charge transfer and polarizability of halogen atom in $F_3CCCl\cdots OCH_2$ and $H_3CCCl\cdots OCH_2$ complexes are important factors, e.g., it is responsible for greater ability of halogen bond formation. On the other hand, using symmetry-adapted perturbation theory (SAPT), Riley and Hobza [30] showed that halogen bonding interactions involving chlorine and bromine atoms are principally dispersive in nature, although electrostatic contributions to halogen bonds are not negligible. In this study, we used EDA calculations based on Kitaura-Morokuma method, which gives energy decomposition terms in good agreement with those of SAPT [60].

Table 3 lists the EDA results for the different DCAA dimers analyzed here. It is evident that for **D1-D3** dimers, the dominant attraction energy originates in the electrostatic term which is about 67 %, 68 % and 64 % of total attractive energy, respectively. This indicates the electrostatic interaction between the DCAA monomers seems to play a large role in determining the geometric structures of these dimers. It should be noted that dipole-dipole interaction forms a part of the first-order electrostatic energy component. The calculated dipole moment value for monomer DCAA (3.11 Debye) shows that this term should be most favorable for **D1** dimer. The hydrogen/halogen-bonded **D4** dimer, with an

Table 3 Interaction energy decomposition scheme for different dimers of DCAA molecules in the gas phase[a]

Dimer	$E_{EL}^{(1)}$	$E_{EX}^{(1)}$	$E_{DEL}^{(R)}$	E_{DISP}	E_{MP2}	$\%E_{EL}^{(1)}$	$\%E_{DEL}^{(R)}$
D1	−30.42	26.54	−11.67	−3.22	−14.8	67	26
D2	−16.79	15.86	−7.11	−0.87	−6.8	68	29
D3	−11.84	11.13	−4.96	−1.57	−5.5	64	27
D4	−14.14	14.97	−12.26	−1.15	−4.9	51	44
D5	−7.44	9.06	−3.8	−1.75	−2.5	57	29
D6	−3.63	4.5	−2.15	−0.93	−1.3	54	32
D7	−5.77	8.02	−2.31	−2.59	−1.3	54	22
D8	−5.85	8.27	−2.41	−2.67	−1.4	53	21
D9	−0.52	1.09	−0.24	−0.73	−0.3	35	16
D10	−3.69	6.35	−1.6	−2.55	−0.7	47	20
D11	−2.3	6.88	−1.47	−3.07	1.3	34	21

[a]All energy components in kcal mol^{-1}.

$E_{EL}^{(1)}$ energy term of -14.14 kcal mol^{-1}, can most closely be compared to the **D5** and **D6** dimers, which have electrostatic energies of -7.44 and -3.63 kcal mol^{-1}, respectively. The interaction between DCAA monomers is dominated by the electrostatic interaction as in the case of the **D1-D3**; nonetheless, delocalization effects play a larger role in the **D4** (44 % of the attractive interaction) than in the **D5** and **D6** (29 % and 32 % of the attractive interaction, respectively). Another important aspect of these data is the fact that for the **D9** dimer, with one Cl Cl contact, the dispersion term amounts to about 50 % of total attractive energy. It is also interesting to note that as the interaction energy of halogen bond decreases, the degree of $E_{EL}^{(1)}$ is expected to decrease. On the other hand, for the halogen-bonded **D5-D11** dimers, about 14–49 % of the total interaction energy is accounted at the HF level and the magnitude of the dispersion energy E_{DISP} has a large effect on the relative magnitudes of the total interaction energy. In summary, the major attractive force in the Cl···Cl and Cl O halogen-bonded dimers is the electrostatic and dispersion interactions, with the former contribution being nearly twice as large as the corresponding contribution from delocalization effects.

Solid phase

In this part, we attempted to investigate the H-bonding and halogen-bonding effects on ^{17}O, ^{35}Cl and ^{2}H NQR parameters of DCAA in the crystalline lattice. Figure 3, which is constructed using X-ray diffraction atomic coordinates [31], shows that DCAA molecule makes a variety of intermolecular interactions in its solid phase. Considering this fact, an eight-molecule cluster was created. Because the cluster model of DCAA was considered, it was expected that the calculated NQR parameters would be close to those quantities which were measured by the experimental devices. The results are summarized in Table 3. The EFG tensor calculations were performed using the B3LYP, CAM-B3LYP, M06, M06-L, M06-2X and wB97XD density functionals with 6-311++G** basis set.

NQR parameters

Table 4 presents the evaluated C_{Q} and η_{Q} parameters at the sites of ^{17}O, ^{35}Cl and ^{2}H nuclei of DCAA in both gas phase and crystalline lattice. At first glance to the calculated results, some interesting trends can be easily obtained. First, for those nuclei participating in the H-bonding and halogen-bonding interactions, NQR parameters exhibit significant changes on going from the isolated molecule model to the target molecule in the cluster. On the other hand, the C_Q values of those nuclei which contribute in the H-bonding interactions decrease, but their η_Q values do not indicate a regular pattern from the isolated gas phase to the cluster. Of course, the magnitude of these changes at each nucleus depends directly on its amount of contribution to the interactions. Second, considering the calculated NQR parameters by 6-311++G** basis set, it is clear that the results are considerably dependent on the density functional used. Considering the evaluated $C_Q(^{17}\mathrm{O})$ values, it is evident that the results obtained by different DFT methods agree with each other to within 0.03–0.80 MHz.

As shown in Fig. 1, there are two crystallographically distinct oxygen sites in DCAA [31]: carboxylic C=O, and hydroxylic O–H. From Table 2, it can be seen that all of the $C_Q(^{17}\mathrm{O})$ values of the monomer DCAA lie within the 8.67–9.59 MHz and that of O–H oxygen is relatively lower than C=O. Clearly, a different C_Q and η_Q values observed for the oxygen sites in monomer DCAA must arise from differences in the surrounding environment. The B3LYP and CAM-B3LYP functionals predict near identical C_Q and η_Q parameters for O1 site of monomer DCAA. The M06 and

Table 4 Calculated NQR parameters (C_Q and η) at the sites of ^{17}O, ^{35}Cl, and ^{2}H nuclei for monomer and octamer cluster of DCAA[a-d]

Nuclei	Parameters	M06	M06-L	M06-2X	B3LYP	CAM-B3LYP	wB97xD	Exp.
O1	C_Q	8.70	8.67	9.03	9.19	9.21	9.09	–
	η	0.52	0.55	0.49	0.51	0.51	0.53	–
O2	C_Q	8.84	9.00	9.46	9.45	9.59	9.41	–
	η	0.22	0.15	0.20	0.24	0.25	0.26	–
Cl1	C_Q	73.53	70.96	77.06	74.93	75.99	74.92	–
	η	0.04	0.04	0.03	0.04	0.03	0.03	–
Cl2	C_Q	73.37	70.93	76.41	74.67	75.70	74.65	–
	η	0.06	0.06	0.07	0.06	0.06	0.06	–
H1	C_Q	297.17	295.61	295.25	293.85	297.86	303.06	–
	η	0.10	0.10	0.11	0.10	0.10	0.10	–
H2	C_Q	198.97	201.07	195.31	197.53	199.34	198.74	–
	η	0.01	0.01	0.01	0.01	0.01	0.01	–
O1	C_Q	7.70	7.69	8.05	8.22	8.18	8.04	7.49
	η	0.23	0.25	0.21	0.20	0.21	0.22	0.22
O2	C_Q	7.80	7.87	8.54	8.36	8.51	8.38	8.21
	η	0.08	0.13	0.07	0.05	0.06	0.05	0.16
Cl1	C_Q	73.83	71.46	76.42	75.79	76.73	75.14	–
	η	0.06	0.05	0.05	0.05	0.04	0.05	–
Cl2	C_Q	73.05	70.63	75.26	74.77	75.50	74.85	–
	η	0.05	0.06	0.05	0.05	0.05	0.06	–
H1	C_Q	187.10	184.23	186.46	199.07	203.02	206.81	182
	η	0.15	0.15	0.16	0.14	0.15	0.15	–
H2	C_Q	192.51	193.30	190.64	197.30	199.11	197.94	–
	η	0.02	0.02	0.02	0.02	0.02	0.02	–

[a]C_Q values for ^{17}O and ^{35}Cl in MHz . [b] C_Q values for ^{1}H in kHz. [c]Experimental NQR parameters for ^{17}O nuclei from ref. [61]. [d] Experimental NQR parameters for ^{2}H nuclei from reference 63

M06-L functionals, on the other hand, considerably underestimate the evaluated C_Q (^{17}O) values, as compared to the others.

In crystalline structure, DCAA molecules are mainly held together in dimers by the familiar carboxylic acid dimeric linkage, involving two symmetry–equivalent HBs (Fig. 4). These are of medium strength, with O···O separation of about 2.63 Å [31]. A quick look at the results reveals that

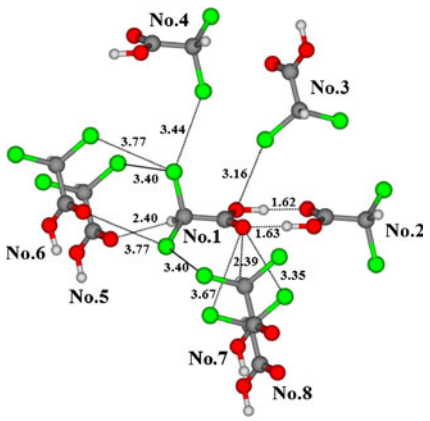

Fig. 4 Crystalline structure of DCAA. Dotted lines show hydrogen/halogen bonding interactions

intermolecular O–H···O interactions affect the calculated ^{17}O NQR parameters at the O1 and O2 sites; however, such an influence is not equivalent for the two oxygen nuclei. As seen in Table 4, M06-2X calculations reveal that the C_Q(O1) parameter decreases by 0.98 MHz depending on whether the DCAA molecule is in the gas phase or in the crystal lattice. On the other hand, the corresponding asymmetry parameter decreases about 0.28 units on going from the single monomer to the target molecule in the cluster. The calculated C_Q parameter for O1 in crystalline DCAA is 8.05 MHz, which is slightly larger than that of α-chloroacetic acid (exp. 7.49 MHz) and acetic acid (exp. 7.28 MHz) [61], but quite smaller than salicylic acid (ca. 9.19 MHz) [62]. In contrast, the ^{17}O NQR parameters at the site of O2 show slightly less sensitivity to the H–bonding interactions. Figure 4 shows that O2 contributes to two HBs, O–H···O (1.63 Å) and C–H···O (2.39 Å), as well as two O···Cl halogen-bonding interactions in crystalline DCAA (3.35 Å and 3.40 Å). Because of the proper H-bonding and halogen bonding distances, C_Q(O2) decreases by 0.92 MHz from the monomer to the target molecule in the cluster. The η_Q also decreases by 0.13 units from the monomer to the cluster. These significant changes reveal the importance of the carboxylic group in contributing to the strong HBs and halogen bonds in the crystalline DCAA.

As evident from Fig. 4, the Cl1 atom of target molecule contributes to the Cl···Cl type halogen-bonding interactions in the crystalline DCAA. For the NQR parameters of this site, the comparison of the isolated model and the octamer cluster shows some discrepancies, although not as dramatic as the one seen for O1 and O2. The M06-2X calculations reveal that the C_Q (^{35}Cl) at the site of Cl1 decreases by only 0.64 MHz from the monomer to the target molecule in the cluster. Besides, the corresponding η_Q value at this site increases by 0.03 (in monomer) to 0.05 (in cluster). On the other hand, Cl2 atom of the target unit interacts with O2 and Cl1 of molecules No. 5 and 7, respectively. From Table 4, it is shown that the evaluated C_Q (^{35}Cl) value decreases by about 1.15 MHz from the monomer to the octamer cluster.

Table 4 shows that the NQR parameters of the carboxylic hydrogen atom (H1) vary considerably between the monomer and octamer cluster, ΔC_Q=109 kHz and $\Delta(\eta_Q)$=0.05 units. The calculated C_Q and η_Q values for H1 of the target molecule are obtained to be 186 MHz and 0.16 units at the M06-2X level, respectively. These values, which are obtained by taking the whole cluster into consideration, are expected to be close to the other carboxylic compounds [63]. From Fig. 1, it is clear that molecule No. 5 is capable of making a weak C–H···O H-bonding with the target molecule, $r_{CH\cdots O}$=2.40 Å, and ∠C-H···O=128°. Because of the unusual nature of C–H···O H-bonding in the biological systems, it is, therefore, of interest to examine the effect of this interaction on the ^{2}H NQR parameters in more detail. As the results of Table 4 illustrate, while the CH···O H-bonding interaction does not affect the asymmetry parameter, it decreases the calculated C_Q(^{2}H) value by 5 kHz. This is in agreement with earlier observations [64, 65] made for this interaction, and is due to the limited involvement of C-H group in the intermolecular interaction of DCAA in its solid phase.

Concluding remarks

In this paper, we performed a systematic computational investigation on the intermolecular HBs and halogen bonds properties in crystalline DCAA by means of DFT calculations and MP2 calculations. Some results are:

1. Electrostatic potential calculation indicated that there is a strong negative potential encompassing the carbonyl oxygen (O2). The very strongly positive electrostatic potential of the hydroxyl hydrogen (H1), $V_{S,max}$= 60.4 kcal mol^{-1}, and the $V_{S,min}$=-30.2 kcal mol^{-1} of the carbonyl oxygen indicate their propensities for non-covalent H-bonding, as a donor and an acceptor, respectively. There is also a smaller and weaker positive region on the outermost portion of each Cl atoms centered about the intersection of its surface with the C–Cl axis.
2. For the DCAA dimers studied here, the evaluated Cl···Cl separations are in a range from 3.56 to 4.00 Å. These separations are slightly longer than the sum of two chlorine vdW radii, 3.50 Å. However, for most of the dimers studied, it has been shown that the optimized equilibrium Cl···O bonds are essentially shorter than the sum of the vdW radii of the Cl and O atoms (3.27 Å), implying an attractive interaction between DCAA monomers.
3. For the O–H···O interactions of **D1**, it can be seen that the values of ρ_{BCP} are calculated to be 0.042 au, whereas the values of $\nabla^2\rho_{BCP}$ are positive (0.142 au). These values are within the common accepted values for H-bonding interactions, thus indicating the closed-shell interactions in DCAA. However, negative values of H_{BCP} are predicted for these HBs, suggesting that the interactions have some degree of covalent character. As is obvious from Table 1, the ellipticity values for the O–H···O interactions are nearly small and zero, indicating that the HBs are conserved in the **D1-D4** structures. Based on QTAIM analysis, it can be said that, the weak C–H···O and H···Cl bonds are similar in character to the halogen bonds found in the DCAA dimers.
4. EDA results indicated that the major attractive force in the halogen-bonded dimers is the electrostatic and dispersion interactions. However, it is evident that for the **D1** dimer, the dominant attraction energy originates in the electrostatic term which is about 67 % of total attractive energy. On the other hand, for all halogen-bonded dimers, about 14-49 % of the total interaction energy is accounted at the HF level and the magnitude of the dispersion energy E_{DISP} has a large effect on the relative magnitudes of the total interaction energy.
5. Our calculations indicate that NQR parameters of ^{17}O, ^{35}Cl, and ^{1}H nuclei in crystalline DCAA are influenced by H–bonding and halogen-bonding interactions and as such are appropriate parameters to characterize the properties of these interactions.

References

1. Woo HK, Wang XB, Wang LS, Lu KC (2005) Probing the low-barrier hydrogen bond in hydrogen maleate in the gas phase: a photoelectron spectroscopy and *ab initio* study. J Phys Chem A 109:10633–10637
2. Hobza P, Havlas Z (2000) Blue-shifting hydrogen bonds. Chem Rev 100:4253–4264
3. Murray JS, Concha MC, Lane P, Hobza P, Politzer P (2008) Blue shifts vs red shifts in σ-hole bonding. J Mol Model 14:699–704
4. Scheiner S (1997) Hydrogen bonding: a theoretical prospective. Oxford University Press, Oxford UK

5. Behzadi H, Esrafili M, Hadipour NL (2007) A theoretical study of 17O, 14N and 2H nuclear quadrupole coupling tensors in the real crystalline structure of acetaminophen. Chem Phys 333:97–103
6. Esrafili MD, Behzadi H, Hadipour NL (2008) 14N and 17O electric field gradient tensors in benzamide clusters: theoretical evidence for cooperative and electronic delocalization effects in N–H···O hydrogen bonding. Chem Phys 348:175–180
7. Desiraju GR, Steiner T (1999) The weak hydrogen bond in structural chemistry and biology. Oxford University Press, New York
8. Richardson TB, de Gala S, Crabtree RH, Siegbahn PEM (1995) Unconventional hydrogen bonds: intermolecular B-H…H-N Interactions. J Am Chem Soc 117:12875–12786
9. Politzer P, Murray JS, Concha MC (2007) Halogen bonding and the design of new materials: organic bromides, chlorides and perhaps even fluorides as donors. J Mol Model 13:643–650
10. Riley KE, Murray JS, Politzer P, Concha MC, Hobza P (2009) Br···O complexes as probes of factors affecting halogen bonding: interactions of bromobenzenes and bromopyrimidines with acetone. J Chem Theor Comput 5:155–163
11. Bent HA (1968) Structural chemistry of donor-acceptor interactions. Chem Rev 68:587–648
12. Hassel O (1970) Structural aspects of interatomic charge-transfer bonding. Science 170:497–502
13. Bernard-Houplain MC, Sandorfy C (1973) Low temperature infrared study of hydrogen bonding in dissolved pyrrole and indole. Can J Chem 51:1075–1082
14. Bernard-Houplain MC, Sandorfy C (1973) A low temperature infrared study of hydrogen bonding in N-Alkylacetamides. Can J Chem 51:3640–3646
15. Metrangolo P, Neukirch H, Pilati T, Resnati G (2005) Halogen bonding based recognition processes: a world parallel to hydrogen bonding. Acc Chem Res 38:386–395
16. Jiang Y, Alcaraz AA, Chen JM, Kobayashi H, Lu YJ, Snyder JP (2006) Diastereomers of dibromo-7-epi-10-deacetylcephalomannine: crowded and cytotoxic taxanes. Exhibit halogen bonds. J Med Chem 49:1891–1899
17. Lopez-Rodriguez ML, Murcia M, Benhamu B, Viso A, Campillo M, Pardo L (2002) Benzimidazole derivatives. 3. 3D-QSAR/CoMFA model and computational simulation for the recognition of 5-HT(4) receptor antagonists. J Med Chem 45:4806–4815
18. Auffinger P, Hays FA, Westhof E, Ho PS (2004) Halogen bonds in biological molecules. Proc Natl Acad Sci USA 101:16789–16794
19. Politzer P, Lane P, Concha MC, Ma YG, Murray JS (2007) An overview of halogen bonding. J Mol Model 13:305–311
20. Clark T, Hennemann M, Murray JS, Politzer P (2007) Halogen bonding: the σ-hole. J Mol Model 13:291–296
21. Murray-Rust P, Motherwell WDS (1979) Computer retrieval and analysis of molecular geometry. 4. Intermolecular interactions. J Am Chem Soc 101:4374–4376
22. Murray-Rust P, Stallings WC, Monti CT, Preston RK, Glusker JP (1983) Intermolecular interactions of the carbon-fluorine bond: the crystallographic environment of fluorinated carboxylic acids and related structures. J Am Chem Soc 105:3206–3214
23. Ramasubbu N, Parthasarathy R, Murray-Rust P (1986) Angular preferences of intermolecular forces around halogen centers: preferred directions of approach of electrophiles and nucleophiles around carbon-halogen bond. J Am Chem Soc 108:4308–4314
24. Politzer P, Murray JS, Concha MC (2008) σ-hole bonding between like atoms; a fallacy of atomic charges. J Mol Model 14:659–665
25. Trogdon G, Murray JS, Concha MC, Politzer P (2007) Molecular surface electrostatic potentials and anesthetic activity. J Mol Model 13:313–318
26. Awwadi FF, Willett RD, Peterson KA, Twamley B (2006) The nature of halogen···halogen synthons: crystallographic and theoretical studies. Chem Eur J 12:8952–8960
27. Metrangolo P, Murray JS, Pilati T, Politzer P, Resnati G (2011) The fluorine atom as a halogen bond donor, viz. a positive site. Cryst Eng Comm 13:6593–6596
28. Metrangolo P, Murray JS, Pilati T, Politzer P, Resnati G, Terraneo G (2011) Fluorine-centered halogen bonding: a factor in recognition phenomena and reactivity. Cryst Growth Des 11:4238–4246
29. Lommerse JPM, Stone AJ, Taylor R, Allen FH (1996) The nature and geometry of intermolecular interactions between halogens and oxygen or nitrogen. J Am Chem Soc 118:3108–3116
30. Riley KE, Hobza P (2008) Investigations into the nature of halogen bonding including symmetry adapted perturbation theory analyses. J Chem Theor Comput 4:232–242
31. Gajda R, Katrusiak A (2007) Compressed hydrogen-bond effects in the pressurefrozen chloroacetic acid. Acta Cryst B63:896–902
32. Schmidt MW, Baldridge KK, Boatz JA, Elbert ST, Gordon MS, Jensen JH, Koseki S, Matsunaga N, Nguyen KA, Su SJ, Windus TL, Dupuis M, Montgomery JA (1993) General atomic and molecular electronic structure system. J Comput Chem 14:1347–1363
33. Wamg W, Hobza P (2008) Origin of the X-Hal (Hal=Cl, Br) bond-length change in the halogen-bonded complexes
34. Zhao Y, Truhlar DG (2008) The M06 suite of density functionals for main group thermochemistry, thermochemical kinetics, noncovalent interactions, excited states, and transition elements: two new functionals and systematic testing of four M06-class functionals and 12 other functional. Theor Chem Acc 120:215–241
35. Boys SF, Bernardi F (1970) The calculation of small molecular interactions by the differences of separate total energies. Some procedures with reduced errors. Mol Phys 19:553–566
36. Bader RFW (1990) Atoms in molecules-a quantum theory. Oxford University Press, New York
37. Biegler-Konig F, Schonbohm J, Bayles D (2001) AIM 2000. J Comput Chem 22:545–559
38. Kitaura K, Morokuma K (1976) A new energy decomposition scheme for molecular interactions within the Hartree-Fock approximation. Int J Quantum Chem 10:325–340
39. Lucken EAC (1990) Nuclear quadrupole coupling constants. Academic, London
40. Pyykkö P (2001) Spectroscopic nuclear quadrupole moment. Mol Phys 99:1617–1629
41. Bader RFW, Carroll MT, Cheeseman JR, Chang C (1987) Properties of atoms in molecules: atomic volumes. J Am Chem Soc 109:7968–7979
42. Bulat FA, Toro-Labbé A, "WFA: A suite of programs to analyse wavefunctions", unpublished
43. Bulat FA, Toro-Labbé A, Brinck T, Murray JS, Politzer P (2010) Quantitative analysis of molecular surfaces: areas, volumes, electrostatic potentials and average local ionization energies. J Mol Model 16:1679–1691
44. Bondi A (1964) Van der Waals volumes and radii. J Phys Chem 68:441–451
45. Koch U, Popelier PLA (1995) Characterization of C-H-O hydrogen bonds on the basis of the charge density. J Phys Chem 99:9747–9754
46. Perlstein J, Steppe K, Vaday S, Ndip EMN (1996) Molecular self-assemblies. 5. Analysis of the vector properties of hydrogen bonding in crystal engineering. J Am Chem Soc 118:8433–8443
47. Lu YX, Zou JW, Wang YH, Jiang YJ, Yu QS (2007) *Ab Initio* investigation of the complexes between bromobenzene and several electron donors: some insights into the magnitude and nature of halogen bonding interactions. J Phys Chem A 111:10781–10788
48. Wang S (2010) Properties of halogen bonds in FArCCX···HMY (X=Cl and Br; M=Be and Mg; Y=H, F, and CH_3) complexes: An *ab initio* and topological analysis. J Mol Struct THEOCHEM 952:115–119

49. Duarte DJ, de las Vallejos MM (2010) Topological analysis of aromatic halogen/hydrogen bonds by electron charge density and electrostatic potentials. J Mol Model 16:737–748
50. Esrafili MD, Hadipour NL (2011) Characteristics and nature of halogen bonds in linear clusters of NCX (X=Cl, and Br): an *ab initio*, NBO and QTAIM study. 109:2451–2460
51. Esrafili MD, Behzadi H, Beheshtian J, Hadipour NL (2008) Theoretical 14N nuclear quadrupole resonance parameters for sulfa drugs: Sulfamerazine and sulfathiazole. J Mol Graphics Modell 27:326–331
52. Rozas I, Alkorta I, Elguero (2000) Behaviour of ylides containing N, O and C atoms as hydrogen bond acceptors. J Am Chem Soc 122:11154–11161
53. Popelier P (2000) Atoms in molecules, an introduction. Prentice Hall, Englewood Cliffs, NJ
54. Murray JS, Lane P, Clark T, Politzer P (2007) σ-hole bonding: molecules containing group VI atoms. J Mol Model 13:1033–1038
55. Brinck T, Murray JS, Politzer P (1993) Molecular surface electrostatic potentials and local ionization energies of Group V–VII hydrides and their anions: relationships for aqueous and gas-phase acidities. Int J Quantum Chem 48:73–88
56. Colominas C, Teixidó J, Cemeli J, Luque FJ, Orozco M (1998) Dimerization of carboxylic acids: reliability of theoretical calculations and the effect of solvent. J Phys Chem B 102:2269–2276
57. Chocholousova J, Vacek J, Hobza P (2003) Acetic acid dimer in the gas phase, nonpolar solvent, microhydrated environment, and dilute and concentrated acetic acid: Ab initio quantum chemical and molecular dynamics simulations. J Phys Chem A 107:3086–3092
58. Salvador P, Simon S, Duran M, Dannenberg JJ (2000) C–H···O H-bonded complexes: how does basis set superposition error change their potential-energy surfaces? J Chem Phys 113:5666–5674
59. Palusiak M (2010) On the nature of halogen bond – The Kohn–Sham molecular orbital approach. J Mol Struct THEOCHEM 945:89–92
60. Langlet J, Caillet J, Bergès RP (2003) Comparison of two ways to decompose intermolecular interactions for hydrogen-bonded dimer systems. J Chem Phys 118:6157–6166
61. Brosnan SGP, Edmonds DT, Poplett IJF (1981) J Magn Reson 45:451–460
62. Poplett JF, Smith JAS (1981) 17O and 2H quadrupole double resonance in some carboxylic acid dimers. J Chem Soc Faraday Trans 277:1473–1485
63. Berglund B, Lindgren J, Tegenfeldt J (1987) On the correlation between deuteron quadrupole coupling constants, O-H and O-D stretching frequencies and hydrogen-bond distances in solid hydrates. J Mol Struct 43:179–181
64. Esrafili M, Behzadi H, Hadipour NL (2008) Density functional theory study of N–H···O, O–H···O and C–H···O hydrogen-bonding effects on the 14N and 2H nuclear quadrupole coupling tensors of N-acetyl-valine. Biophys Chem 133:11–18
65. Ida R, Clerk MD, Wu G (2006) Influence of N-H···O and C-H···O hydrogen bonds on the 17O NMR tensors in crystalline uracil: computational study. J Phys Chem A 110:1065–1071